THE JOURNAL OF BIOLOGICAL CHEMISTRY VOL. 286, NO. 33, pp. 29086–29097, August 19, 2011

Mouse Knockout of the Cholesterogenic Cytochrome P450 Lanosterol 14α-Demethylase (*Cyp51*) Resembles Antley-Bixler Syndrome*[S]

Received for publication, April 20, 2011, and in revised form, June 24, 2011 Published, JBC Papers in Press, June 25, 2011, DOI 10.1074/jbc.M111.253245

Rok Keber[‡1], Helena Motaln[‡§1], Kay D. Wagner[¶‖], Nataša Debeljak[‡‡], Minoo Rassoulzadegan[‖], Jure Ačimovič[‡‡], Damjana Rozman[‡‡], and Simon Horvat[‡§§2]**

*From the [‡]Department of Animal Science, Biotechnical Faculty, University of Ljubljana, [‡‡]Institute of Biochemistry, Centre for Functional Genomics and Bio-Chips, Faculty of Medicine, University of Ljubljana, the [§]Department of Genetic Toxicology and Cancer Biology, National Institute of Biology, and the [§§]National Institute of Chemistry, 1000 Ljubljana, Slovenia and [¶]INSERM U907, [‖]Université de Nice, Sophia-Antipolis, and the **Centre de Biochimie, INSERM U636, Parc Valrose, Nice, France*

Antley-Bixler syndrome (ABS) represents a group of heterogeneous disorders characterized by skeletal, cardiac, and urogenital abnormalities that have frequently been associated with mutations in fibroblast growth factor receptor 2 or cytochrome P450 reductase genes. In some ABS patients, reduced activity of the cholesterogenic cytochrome P450 CYP51A1, an ortholog of the mouse CYP51, and accumulation of lanosterol and 24,25-dihydrolanosterol has been reported, but the role of *CYP51A1* in the ABS etiology has remained obscure. To test whether *Cyp51* could be involved in generating an ABS-like phenotype, a mouse knock-out model was developed that exhibited several prenatal ABS-like features leading to lethality at embryonic day 15. *Cyp51*$^{-/-}$ mice had no functional *Cyp51* mRNA and no immunodetectable CYP51 protein. The two CYP51 enzyme substrates (lanosterol and 24,25-dihydrolanosterol) were markedly accumulated. Cholesterol precursors downstream of the CYP51 enzymatic step were not detected, indicating that the targeting in this study blocked *de novo* cholesterol synthesis. This was reflected in the up-regulation of 10 cholesterol synthesis genes, with the exception of 7-dehydrocholesterol reductase. Lethality was ascribed to heart failure due to hypoplasia, ventricle septum, and epicardial and vasculogenesis defects, suggesting that *Cyp51* deficiency was involved in heart development and coronary vessel formation. As the most likely downstream molecular mechanisms, alterations were identified in the sonic hedgehog and retinoic acid signaling pathways. *Cyp51* knock-out mice provide evidence that *Cyp51* is essential for embryogenesis and present a potential animal model for studying ABS syndrome in humans.

Cholesterol is a structural component of membranes, as well as a precursor for bile acid and steroid hormone synthesis (1). It plays an essential role in development as it is required to bind and activate the morphogenic sonic hedgehog (SHH)[3] (2, 3) and retinoic acid (RA) (4) signaling pathways during early gestation. A relatively high number of human birth defects have been shown to be disorders of metabolism caused by mutations of enzymes mediating cholesterol biosynthesis (reviewed in Refs. 5 and 6). ABS (7) represents a heterogeneous pool of disorders in sterol and steroid metabolism. Clinical features include brachycephaly, facial hypoplasia, bowed ulna or femur, synostosis of the radius, camptodactyly, and cardiac and urogenital abnormalities. ABS is a genetically heterogeneous disorder for which mutations in two causal genes have been identified thus far. Recessive mutations in the cytochrome P450 reductase (*POR*) gene (8–10) are frequently found in an ABS form that includes disordered steroidogenesis (ABS1; MIM201750). A predominantly skeletal phenotype without genital anomalies or disordered steroidogenesis can be caused by a dominant mutation in a fibroblast growth factor receptor 2 gene, *FGFR2* (ABS2; MIM 207410). However, ABS-like phenotypes have also been reported in response to fluconazole, an inhibitor of fungal CYP51 used to treat fungal infections. High-dose fluconazole exposure during early pregnancy resulted in inhibition of the *CYP51A1* gene product and ABS-like defects in four reported cases (11–13). Two ABS case studies reported impaired CYP51 activity and markedly increased levels of lanosterol and 24,25-dihydrolanosterol, substrates of CYP51 (14). However, a direct causative CYP51-ABS relationship has not yet been proven in any of the aforementioned cases.

Lanosterol 14α-demethylase (in humans CYP51A1; in mouse, CYP51) is the most evolutionarily conserved member of the cytochrome P450 superfamily (15) and is present in all phyla. It has been studied in many species, including human (16), mouse (17), and fungi where it represents a target for azoles (18). The enzyme catalyzes demethylation of lanosterol or 24,25-dihydrolanosterol in the cholesterol synthesis pathway using POR as an obligatory redox partner (16). To test whether *Cyp51* deficiency can cause an ABS-like phenotype, and to assess the phenotypic effects of CYP51 ablation, we gen-

* This work was supported by grants from the Association pour la Recherche sur le Cancer and Fondation Coeur et Artères (to K. D. W.), and Slovenian Research Agency for core funding program P4-0220 and project 878 and project Syntol (to S. H.), program P4-0104 and projects J1-9438 and J2-2197 (to D. R.), a post-doctoral fellowship (to H. M.), and young researcher Ph.D. scholarship (to R. K.).

[S] The on-line version of this article (available at http://www.jbc.org) contains supplemental Tables S1–S3 and Figs. S1 and S2.

[1] Both authors contributed equally to this work.

[2] To whom correspondence should be addressed: Dept. of Animal Science, University of Ljubljana, Biotechnical Faculty, Groblje 3, Domzale 1230, Slovenia. Tel.: 386-31-331-264; Fax: 386-7217-888; E-mail: simon.horvat@bf.uni-lj.si.

[3] The abbreviations used are: SHH, sonic hedgehog; RA, retinoic acid; ABS, Antley-Bixler syndrome; ES cell, embryonic stem cell; qRT, quantitative reverse transcription; HMGCR, 3-hydroxy-3-methylglutaryl-CoA reductase; E, embryonic day; PCR, polymerase chain reaction.

erated a *Cyp51*$^{-/-}$ mouse knock-out model. *Cyp51* knock-out mice show ABS-like features with skeletal and cardiac malformations leading to embryonic lethality in the late-midgestation period. As the most likely downstream molecular mechanisms, we identified alterations in the SHH and RA signaling pathways.

EXPERIMENTAL PROCEDURES

Generation of Cyp51$^{-/-}$ *Knock-out Mice*—The *Cyp51* homology arm fragments for the targeting construct were isolated from the bacterial artificial chromosome clone 519E21 that was identified in the mouse bacterial artificial chromosome library prepared from 129/Sv genomic DNA (Research Genetics, Huntsville, AL). The targeting construct also contained a thymidine kinase negative selection cassette, a phosphoglycerate kinase-neomycin positive selection cassette flanked by *FRT sites* (*FRT*-neo-*FRT*) inserted in intron 3, and *loxP* sites together with a new HindIII restriction site in introns 2 and 4 (Fig. 1*A*). The linearized construct was electroporated into ES cells isolated from mouse strain 129 (19). After double selection with G418 and ganciclovir, targeted clones carrying the *Cyp51*$^{flox\text{-}FRT\text{-}neo}$ allele were identified using PCR in the 3LoxP, 5LoxP, and neo region as shown in Fig. 1*A* (primers used for genotyping: 3loxF, 5′-AACATAGCCCACTTTAAGCA-3′; 3loxR, 5′-TTCCGCACCTACTGTATTTT-3′; 5loxF, 5′-CAGACTTGATGGCAAGAGAT-3′; 5loxR, 5′-TTAGCTTTAGTCCGTTGCTC-3′; 3NeoF, 5′-AGGATTGGGAAGACAATAGC-3′; 3NeoR, 5′-CTAAAGCGCATGCTCCAG-3′; 5NeoF, 5′-CTGATCTTTGCTGTTGTGG-3′; 5NeoR, 5′-CTAAAGCGCATGCTCCAG-3′). Homologous recombination was confirmed by Southern blot analysis (Fig. 1*B*) on HindIII- and BamHI-digested ES clone genomic DNA using probes located outside the 5′ and 3′ homology arms. Probes were labeled with [^{32}P]dCTP in a random priming reaction using the RediPrime II DNA labeling system (Amersham Biosciences). The phosphoglycerate kinase-neomycin cassette was excised from the *Cyp51*$^{flox\text{-}FRT\text{-}neo}$ ES clones by electroporating a eukaryotic expression vector encoding the FLP recombinase to generate a conditional *Cyp51*^{flox} allele. Correct excision of the selection cassette in ES cells was confirmed by PCR (using the 5Neo and 3Neo primer pairs) and sequencing across all important elements. Mouse chimeras were generated by injecting two independently targeted *Cyp51*^{flox} ES clones into C57BL/6JOlaHsd (C57BL/6; Harlan, Italy) mouse blastocysts. Heterozygous *Cyp51*$^{+/flox}$ offspring were backcrossed to C57BL/6 for at least four generations to generate the transgenic line B6;129SV^{Cyp51tm1Bfro}. The *Cyp51*^{flox} allele was detected in segregating progeny by PCR from ear clips using the 3loxF and 3loxR primers (Fig. 1*C*). The knock-out mouse line B6;129SV$^{Cyp51tm1.1Bfro}$ carrying the *Cyp51*$^{-}$ allele lacking exons 3 and 4 was generated by crossing homozygous *Cyp51*$^{flox/flox}$ females with transgenic males carrying *EIIa-Cre* (strain B6.FVB-Tg(EIIa-cre)C5379Lmgd/J, Jackson Laboratories). To obtain knock-out embryos, F_1 *Cyp51*$^{+/-}$ mice were set up for mating at the end of the light cycle period. The day a vaginal plug was detected was designated embryonic day 0.5 (E0.5). Pregnant females at E9.5, E10.5, E11.5, E12.5, E13.5, and E14.5 were sacrificed with cervical dislocation, and embryos were isolated in PBS. After photographing, leg tissue of the embryos was dissected away for PCR genotyping (Fig. 1, *D* and *E*), and the rest of the embryos were processed for paraffin embedding using standard protocols. Subsequent sections (5 μm) were used for hematoxylin and eosin staining and histology analysis. Alcian staining of E14.5–E15.0 embryos was performed as previously described (20). The Chi-square test was used to compare the observed frequencies in genotypic classes with the expected 1:2:1 F_2 Mendelian ratio. All animal experiments were performed in accordance with institutional guidelines and were approved by the Veterinary Administration of the Republic of Slovenia.

Immunohistochemistry and in Situ Hybridization—Immunohistological studies using paraffin sections of staged mouse embryos were performed according to our previously published protocols (21) using a goat polyclonal anti-platelet/endothelial cell adhesion molecule-1 antibody (Santa Cruz Biotechnology, Santa Cruz, CA) or mouse monoclonal anti-connexin-43 (Transduction Laboratories, Lexington, KY). BrdU incorporation as a measure of cell proliferation was detected as described (22). Terminal deoxynucleotidyltransferase-mediated dUTP nick end labeling (TUNEL) analysis was performed as described (21). For *in situ* hybridization experiments, the GenPoint^{TM} Amplified Detection System (Dako, Carpinteria, CA) was employed using a previously described protocol (24). All plasmids for SHH pathway *in situ* hybridization probes were kindly provided by G. Fishell.

Measurements of Cholesterol Synthesis Intermediates—Quantitative analysis of nine cholesterol precursors and sterols was performed on F_2 embryos of all three genotypes at E12.5 and E14.5 using a gas chromatographic/mass spectrometric method exactly as described (25).

Western Blot Analysis—Frozen E14.5 embryos were pulverized and homogenized with a Polytron homogenizer in lysis buffer (5 mM Tris, pH 7.4, 2 mM EDTA, protease inhibitor mixture (Roche Diagnostics)). The homogenate was centrifuged 15 min at 500 × *g* and 4 °C to remove cell debris. The supernatant was collected and centrifuged 15 min at 45,000 × *g* and 4 °C. The pelleted membrane fraction was resuspended in resuspension buffer (75 mM Tris, 12.5 mM $MgCl_2$, 5 mM EDTA, protease inhibitor mixture). Total protein was measured using the Bradford assay and 40 μg of total protein was loaded onto SDS-PAGE gels. Isolated recombinant bovine CYP51A (55 kDa, ortholog of human CYP51A1 and mouse CYP51) was used as a positive control. Samples were separated by 14% SDS-PAGE for 60 min at 120 V and transferred onto a PVDF membrane (Millipore, Eschborn, Germany) for 2 h at 200 mA (Bio-Rad). After blocking overnight with 5% (w/v) nonfat dry milk in PBST containing 0.05% (v/v) Tween 20, the membrane was incubated for 2 h with rabbit polyclonal anti-CYP51 antibodies (1:500) and anti β-actin antibodies (1:200, Sigma). The anti-CYP51 antibody against the CYP51 peptide QRLKDSWAERLDFNPDRY recognizes several mammalian CYP51 proteins.[4] After three washes for 10 min each in PBST, the membrane was incubated for 2 h with goat anti-rabbit IgG peroxidase, diluted 1:2000 with

[4] D. Rozman, M. Cotman, K. Fon-Tacer, and M. Seliskar, unpublished data.

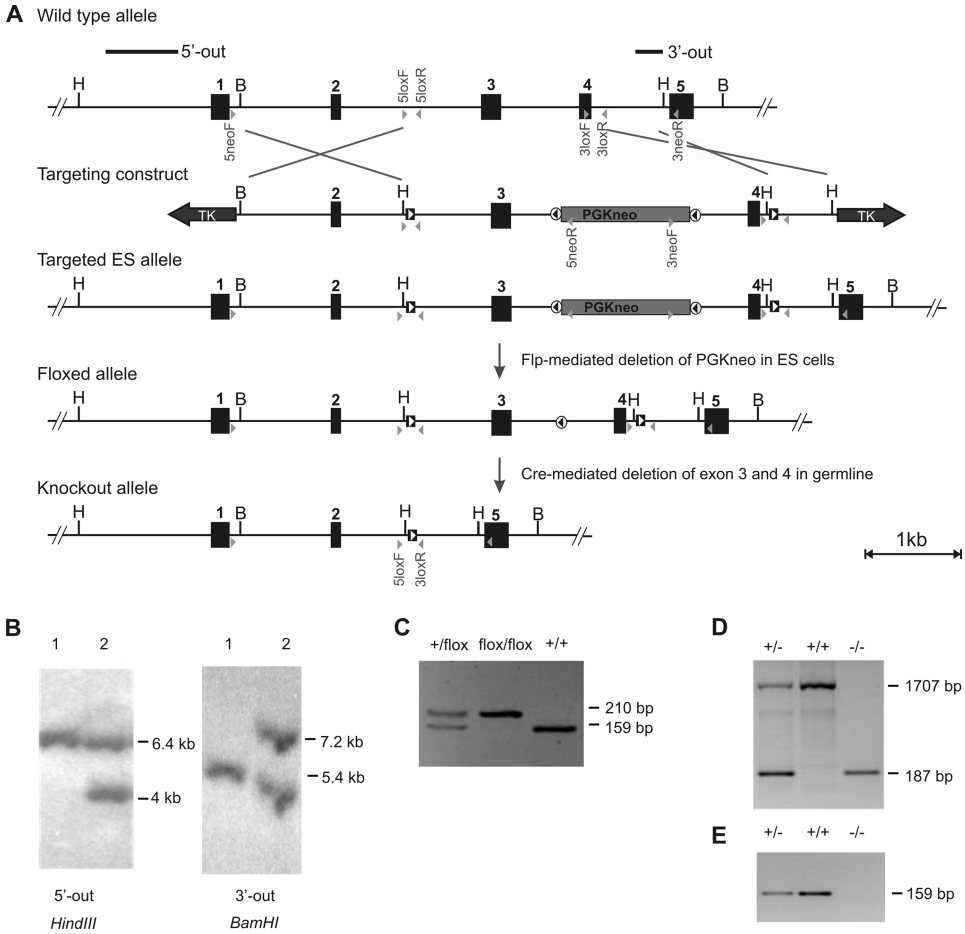

FIGURE 1. **Generation of *Cyp51*$^{-/-}$ mice.** *A,* targeting strategy. The neomycin resistance cassette (*gray box*) flanked with two *FRT* sites (*encircled black triangle*) was inserted into intron 3. Exons 3 and 4 (*black boxes*) were flanked by two *loxP* sites (*squared white triangle*) inserted into introns 2 and 4 (together with new Hin*dIII* restriction sites). The thymidine kinase (*TK*) gene (*gray arrows*) was used for negative selection of non-targeted insertion events. Diagnostic Hin*dIII* (*H*) and Bam*HI* (*B*) restriction sites as well as probes for Southern analysis (*black bars*) located 5′ (5′-out) and 3′ (3′-out) to both homology arms are indicated. *Gray arrows* show PCR primer positions used for genotyping. *Crossed bars* indicate homologous recombination. The neomycin selection cassette was removed in ES cell clones with Flp recombinase generating a conditional *Cyp51*^{flox} allele. EIIa-Cre recombinase was used to obtain the knock-out *Cyp51*$^{-}$ allele lacking exons 3 and 4. *B,* Southern blot of Hin*dIII*- or Bam*HI*-digested DNA from ES cell clones carrying one *Cyp51*$^{flox\text{-}FRT\text{-}neo}$ allele hybridized with 5′-out and 3′-out probes, respectively. *Lane 1* shows wild-type ES cells. *Lane 2* shows a targeted ES cell line. *C,* ear clip DNA genotyping of F_2 offspring carrying the conditional *Cyp51*^{flox} allele using 3loxF/3loxR primers. *D,* PCR genotyping of F_2 embryos carrying knock-out *Cyp51*$^{-}$ allele using 5loxF/3loxR primers. A 187-bp fragment indicates *Cyp51*$^{-}$ allele. *E,* the full knock-out *Cyp51*$^{-/-}$ genotype was further confirmed by the absence of a 159-bp fragment in the 3loxF/3loxR PCR screen. Wild-type, floxed, and knock-out *Cyp51* alleles are designated +, flox and −, respectively.

5% nonfat dry milk in PBST. The membrane was visualized using the enhanced chemiluminescence detection system (ThermoScientific, Rockford, IL) and detected with a camera (Fujifilm LAS-400, Valhalla, NY).

Quantitative RT-PCR—Total RNA was extracted from embryos or embryo hearts using TRIzol reagent (Invitrogen). Total RNA (2.5 or 1 (in hearts) μg) was treated with amplification grade DNase I, and reverse transcribed with the SuperScript® VILO™ cDNA Synthesis Kit (Invitrogen). Real-time quantitative PCR was performed using a LightCycler 480 detection system using SYBR Green I Master, Probes Master for SYBR Green, or TaqMan chemistry according to the manufacturer's instructions (Roche Applied Science). Primers were designed using the Primer Express 1.5 software and validated for PCR efficiency. PCR was performed with the following PCR parameters: 95 °C for 10 min, then 95 °C for 10 s, 60 °C for 30 s, and 72 °C for 5 s for 45 cycles plus a dissociation step (60–95 °C). The relative expression ratios were calculated as described (26). Actin β (*Actb*), glyceraldehyde-3-phosphate dehydrogenase (*Gapdh*), hypoxanthine guanine phosphoribosyl transferase (*Hprt1*) or *Actb,* ribosomal protein, large, P0 (*Rplp0*), UTP6, small subunit processome component, homolog (yeast) (*Utp6c*) were selected as described (27) and used as internal reference genes in embryo hearts and whole embryos, respectively. RNAs for three different mouse *Cyp51* exons were also quantified using TaqMan® Assay-on-Demand gene expression assays and a *β-actin* TaqMan Pre-Developed Assay (Applied Biosystems, Foster City, CA) were used as internal controls. Relative expression was calculated with the standard $\Delta\Delta C_t$ method and analyzed with GraphPad software. The list of primers and pre-developed assays used in quantitative RT-PCR is provided under supplemental Tables S2 and S3.

RESULTS

Generation of Cyp51 Knock-out Mice—We generated a conditional knock-out *Cyp51*^{tm1Bfro} allele of the mouse *Cyp51* gene, referred to here as the *Cyp51*^{flox} allele (MGI: 4357830), by placing two *loxP* sites in introns 2 and 4 of *Cyp51* (Fig. 1). A

deletion of exons 3 and 4 should shift the reading frame in the *Cyp51* transcript generating a premature stop codon and truncated CYP51 protein. There is no evidence for alternative splicing of *Cyp51* or multiple CYP51 proteins in mice or other mammals, although an additional transcript in the testis arising from alternative poly(A) signal selection does exist in several mammalian species. Our knock-out strategy was designed to create null alleles for both the somatic and the shorter testis-specific transcript, because both *Cyp51* poly(A) signals are located downstream from the chosen recombination event in exons 3 and 4. Germline founders carrying the $Cyp51^{flox}$ allele were backcrossed to C57BL/6JOlaHsd mice for at least four generations and then to the EIIa-Cre deleter line mice to generate knock-out $Cyp51^{tm1.1Bfro}$ allele mice, referred to here as the $Cyp51^{-}$ allele (MGI: 4836362). Heterozygous $Cyp51^{+/-}$ mice were intercrossed to obtain homozygous $Cyp51^{-/-}$ knock-out embryos.

To test the pattern of RNA transcription from the *Cyp51* knock-out allele in various parts of the *Cyp51* locus, we performed a quantitative RT-PCR (qRT-PCR) analysis with probes covering exons 1–2, 3–4, and 8–9 in embryos at E12.5 and E14.5 (Fig. 2*A*). $Cyp51^{-/-}$ embryos did not express exons 3 and 4, as expected, given that this segment should have been deleted. From the knock-out allele, there was ~30% transcription of non-coding exons 1 and 2, and 20% of exons 8 and 9 compared with the 100% wild-type allele transcription level. However, as deletion of exons 3 and 4 generates a premature stop codon, any remnant read-through transcription would generate a truncated transcript, as well as a protein devoid of the cysteine-binding site in exon 10 that is crucial for CYP51 activity. Our Western blot analysis (Fig. 2*B*) supports the above *Cyp51* mRNA analysis and demonstrates that there is no immunodetectable CYP51 protein, even in the truncated form, in $Cyp51^{-/-}$ embryos. Therefore, our assays at the DNA, RNA, and protein levels demonstrate that gene targeting was successful in generating a complete loss of function *Cyp51* allele.

Quantification of mRNA and Cholesterol Precursors from the Cholesterol Biosynthesis Pathway of F_2 Embryos—We quantified mRNA expression of 11 genes from the cholesterol biosynthesis pathway and nine intermediates from lanosterol to cholesterol. A deletion of one functional *Cyp51* allele in embryos at E14.5 resulted in a statistically significant decrease of *Cyp51* mRNA, whereas other cholesterogenic genes did not differ significantly between heterozygotes and wild-type (Fig. 3*A*). The sterol measurements in embryos at the same stage corroborate the above mRNA analyses in heterozygous embryos (Fig. 3*B*). Interestingly, in $Cyp51^{-/-}$ embryos, where both *Cyp51* alleles were nonfunctional, expression of all cholesterogenic genes except 7-dehydrocholesterol reductase (*Dhcr7*) was significantly increased. The major accumulating sterol in $Cyp51^{-/-}$ embryos was confirmed to be 24,25-dihydrolanosterol. Cholesterol synthesis intermediates downstream of the CYP51 reaction step were not detected in $Cyp51^{-/-}$ embryos (Fig. 3*B*) demonstrating that a complete block in the cholesterol synthesis pathway occurred in $Cyp51^{-/-}$ knockouts. These embryos nevertheless contained measurable amounts of the final product, cholesterol, although significantly less than wild-type and

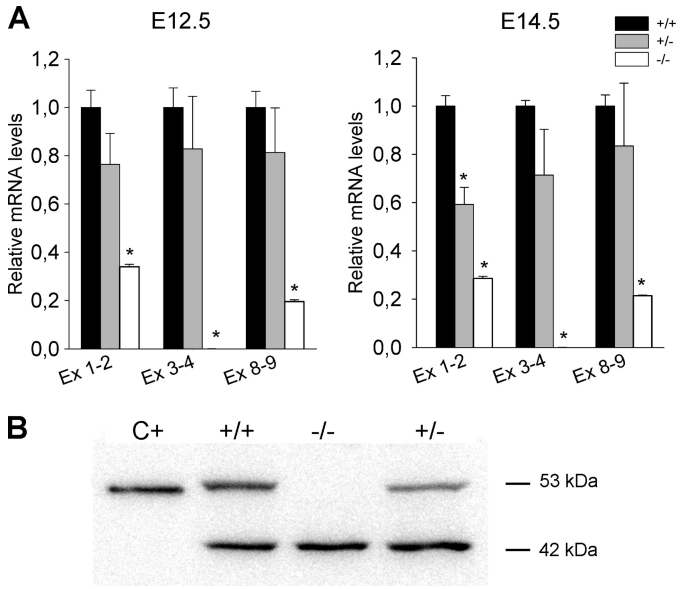

FIGURE 2. ***Cyp51* knock-out embryos did not express functional *Cyp51* mRNA and produced no immunodetectable CYP51 protein.** *A,* quantification of mRNA of various *Cyp51* exons in F_2 embryos. To test the expression pattern of the *Cyp51* knock-out allele in various parts of the *Cyp51* locus, a qRT-PCR analysis was performed on probes covering exons 1 to 2 (*Ex 1–2*), exons 3 to 4 (*Ex 3–4*), and exons 8 to 9 (*Ex 8–9*) in embryos at E12.5 (*left panel*) and E14.5 (*right panel*). *Cyp51* knock-out embryos did not express exons 3 to 4 (this segment was deleted) but retained ~30% transcription of exons 1 to 2 and 20% of exons 8 to 9. Heterozygotes expressed all tested *Cyp51* exons at levels between 60 and 80% of the wild-type. *Bars* show mean ± S.E. ($n = 4$); *, $p < 0.05$. *B, Cyp51* knock-out embryos did not express the CYP51 protein. Membrane protein isolates (40 μg) from E14.5 embryos of the three F_2 genotypes were probed with anti-CYP51 and anti-β-actin antibodies. Western blot demonstrated that there is no immunodetectable CYP51 protein (53-kDa band) in the *Cyp51* knock-out embryos, whereas it is observed in the wild-type and heterozygotes. Isolated recombinant bovine CYP51 was used as a positive control (*lane C+*) for CYP51 detection and β-actin as a loading control (42-kDa). Wild-type, heterozygous, and knock-out embryos are designated +/+, +/−, and −/−, respectively.

heterozygotes. RNA expression analyses and sterol measurements showed similar trends at stage E12.5 (data not shown).

Cyp51 Knock-out Causes an ABS-like Phenotype and Results in Midgestation Lethality—No viable $Cyp51^{-/-}$ mice were identified among 185 weaned progeny derived from heterozygous matings. The ratio of $Cyp51^{+/+}$ and $Cyp51^{+/-}$ adult mice did not deviate significantly from the expected 1:2 Mendelian ratio indicating that lethality did not occur among heterozygotes. To determine the developmental stage of lethality, embryos were genotyped at seven different embryonic stages from E9.5 to E15.5 (Table 1). The results presented in Table 1 were pooled for two lines derived from two independently targeted embryonic stem cell clones, as both lines gave identical outcomes (supplemental Table S1). Genotype ratios from E9.5 to E14.5 were in accordance with the expected F_2 Mendelian ratios. At stage E15.5, however, all $Cyp51^{-/-}$ embryos were in an advanced stage of resorption. Examples of embryos in earlier stages of resorption from different developmental points are presented under supplemental Fig. S1. As the majority of $Cyp51^{-/-}$ embryos at E13.5 and E14.5 (37 out of 41) still had a beating heart, whereas none could be noted at E15.5, we conclude that lethality of the $Cyp51^{-/-}$ embryos occurred at E15. Loss of *Cyp51* function resulted in several developmental malformations. Knock-out embryos were first distinguished at

E10.5 by kinked, shortened tails (*arrow* in Fig. 4*A*) and embryos displayed an increased nuchal translucence most clearly distinguished at E14.5. Severe cases of nuchal translucence were accompanied by hematomas in the dorsolateral and pericardial regions (Fig. 4*B*). Transverse histological sections of nuchal regions demonstrated a highly expanded jugular lymph sac, up to 20 times larger compared with wild-type structures (Fig. 5*A*). Close examination of endothelial cells lining the lymph sacs showed no obvious changes in endothelial cell morphology, but an increase in the number of surrounding smooth muscle cells (Fig. 5*B*). Skeletal abnormalities assessed at E14.5 exhibited shortened fore and hind limbs in all examined specimens (micromelia). The radius and tibia were bowed and synostosis of the femur and tibia was observed (Fig. 4*D*). Tarsal and carpal elements were underdeveloped and distal phalanges were absent. Compared with the forelimbs, the abnormalities in hind limbs were more pronounced and variable in severity between *Cyp51*$^{-/-}$ embryos (Fig. 4*C*). Forelimbs displayed digital joint contractures (campodactyly) resulting in soft tissue syndactyly of the second and third fingers. A differential phenotype between the left and right hind limbs appeared in approximately half of embryos. The third distal tarsal element was absent from both hind limbs resulting in syndactyly of the second and third metatarsal bones on the left foot and the second, third, and fourth metatarsal bones on the right foot. Bone syndactyly of the second and third right metatarsus was complete, whereas the fourth metatarsus was joined only proximally. Proximal hind limb phalanges bifurcated and formed additional fingers (Fig. 4*E*). Histological examination of embryos from different stages revealed an absence of the palatal shelf cartilage resulting in cleft palate (Fig. 4*F*). Knock-out embryos also exhibited some craniofacial abnormalities, including brachycephaly, micrognathia (shortened mandible), and shortened or absent tongue (Fig. 4, *F* and *G*).

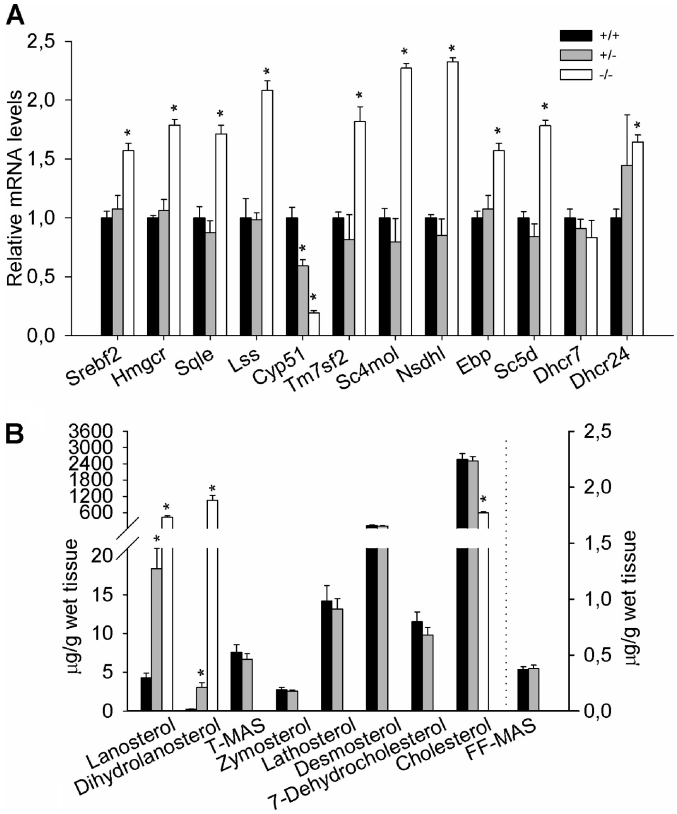

FIGURE 3. **Quantification of cholesterogenic gene expression and sterol intermediates in F_2 embryos at E14.5.** *A,* gene expression in embryos at E14.5. *Cyp51* knock-out embryos exhibited significant increases in mRNA of all cholesterogenic genes, with the exception of *Dhcr7*. In knock-out embryos, there was ~20% read-through transcription of the truncated *Cyp51* transcript compared with the 100% wild-type allele (see Fig. 2). Heterozygous embryos displayed a significant decrease in *Cyp51* expression, whereas the expression of other cholesterogenic genes was not affected. *B,* quantification of sterol intermediates in embryos at E14.5. Upstream intermediates (lanosterol and 24,25-dihydrolanosterol) were highly accumulated in knock-out embryos, significantly increased in heterozygotes, but barely detectable in wild-type embryos. Cholesterol intermediates downstream of the CYP51 catalytic step were below the limit of detection in the *Cyp51* knock-out embryos (no values) compared with heterozygous and wild-type embryos. High amounts of 24,25-dihydrolanosterol and lanosterol masked the measurements of low amounts of other sterols in the GC-MS method. A significant decrease in cholesterol levels was found in knock-out embryos. These results demonstrate a block of *de novo* cholesterol biosynthesis in *Cyp51* knock-out embryos. Quantity of FF-MAS is shown on the *right axis*. *Bars* show mean ± S.E. ($n = 4$), *, $p < 0.05$. *Cyp51* wild-type, heterozygous and knock-out embryos are designated +/+, +/−, and −/−, respectively.

Cyp51 Knock-out Lethality Occurs Most Likely Due to Heart Failure—Macroscopically visible pericardial bleeding was the first sign of heart failure in E14.5 knock-out embryos (Fig. 5*C*). In addition, *Cyp51*$^{-/-}$ embryos exhibited increased nuchal translucence that has been frequently associated with congenital heart defects or underdevelopment of the lymphatic system resulting in overdistension of the jugular lymphatic sacs in humans (reviewed in Ref. 28). In agreement with the human situation, we observed a dramatic jugular lymph sac extension in the knock-out embryos (Fig. 5*A*). Whole mount analysis of the hearts at E14.5 revealed smaller hypoplastic hearts with dilation of the atria, a very prominent interventricular groove, which might result from abnormal development of the inter-

TABLE 1

Genotype frequency analysis of F_2 offspring from *Cyp51*$^{+/-}$ heterozygote crosses

No homozygous *Cyp51*$^{-/-}$ pups were present among 185 screened. Embryo analysis showed lethality betwen stage E14.5 and E15.5 where live *Cyp51* knockouts were no longer present. *p*-values of stages where significant difference from the expected Mendelian ratio was deteceted are underlined. Examples of embryos in early stage of resorbtion from different developmental points are presented under supplemental Fig. S1.

Embryo age	+/+	+/−	−/−	Total	*p* (chi square)	Resorbed[a]
E9.5	0	5	3	8	0.253	2
E10.5	18	30	17	65	0.812	9
E11.5	19	40	22	81	0.889	8
E12.5	32	77	28	137	0.309	14
E13.5	19	39	17	75	0.892	6
E14.5	32	60	24	116	0.537	10
E15.5	8	20	0	28	**0.008**	17
Postnatal	63	122	0	185	**3.95×10^{-14}**	NA[b]

[a] Genotyping of most embryos in advanced stages of resorption was ambiguous because of small amount and degraded DNA and hence no genotype could be ascribed.
[b] NA, not applicable.

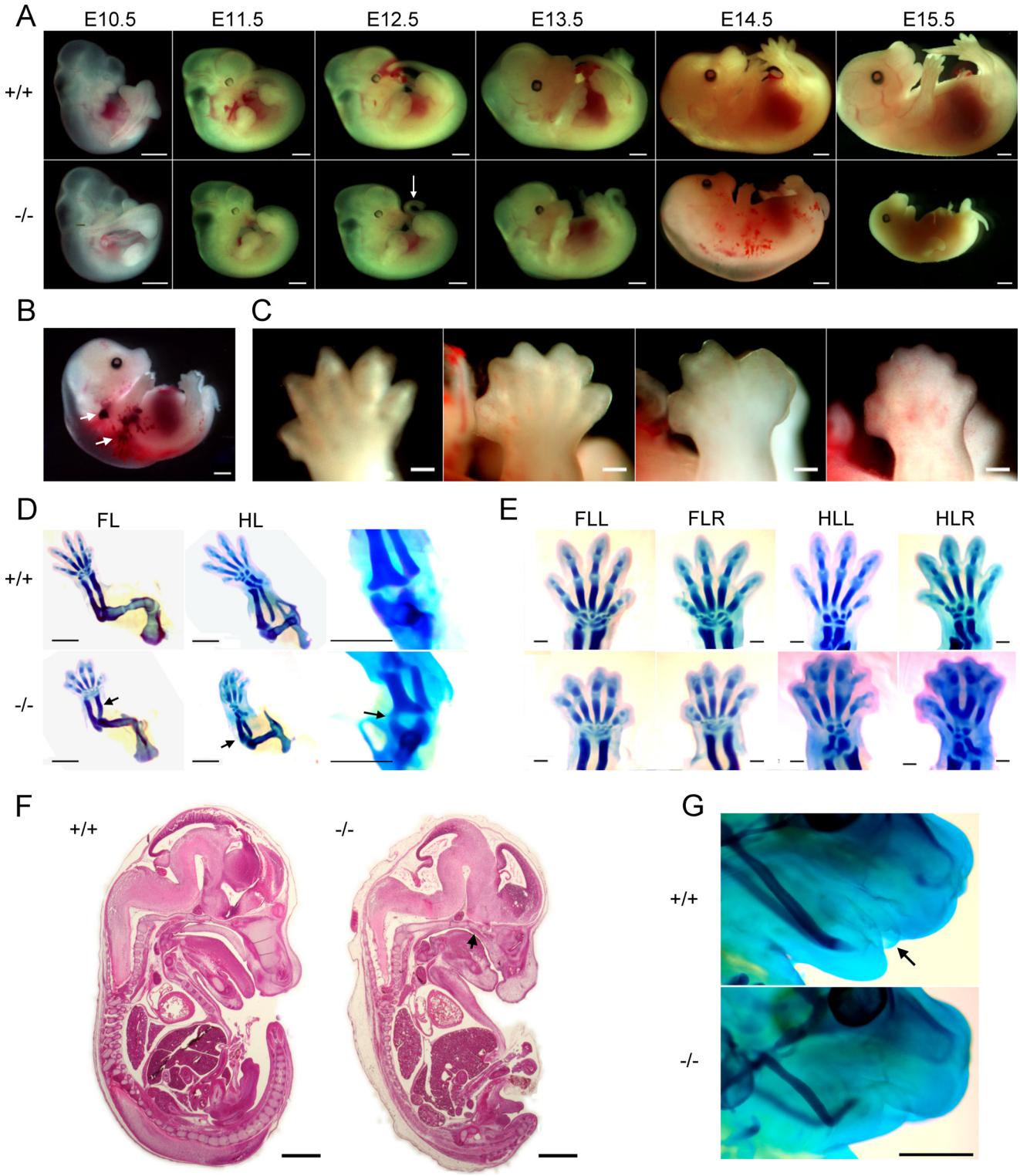

FIGURE 4. **Morphological developmental abnormalities in *Cyp51* knock-out embryos.** *A, Cyp51* knock-out embryos were first distinguished at E11.5–E12.5 by kinked and short tails (*arrow*). Nuchal translucence extending dorsolaterally from the nuchal region was observed in knock-out embryos from stage E12.5 to lethality that occurred at E15.0. At stage E15.5, all knock-out embryos were in an advanced stage of resorption (right most knock-out embryo). *B,* example of nuchal translucence with hemorrhages (*arrow*) at E14.5. *C,* variable phenotypes, ranging from mild to severe (left-right), of soft tissue syndactyly in the right hindlimb at E14.5. *D,* representative limb skeletal abnormalities demonstrated by Alcian blue dye staining. Micromelia (shortened limbs) was observed in all examined specimens. Radius and tibia were shortened and bowed (*arrows*). High magnification demonstrated signs of femuro-tibial synostosis (*arrow*). *E,* tarsal and carpal elements were underdeveloped and distal phalanges were absent. Joining of fingers or toes (syndactyly) was a prominent feature as well as post-axial polydactyly. Camptodactyly was most obvious in the left forelimb. *FL*, forelimb; *HL*, hindlimb (left/right). *F,* gross histological examination of embryos at E14.5. Extended subcutaneous, underdevelopment of tongue, and absence of palatal shelf bone (*arrow*) was visible in knock-out embryos. *G,* the most prominent head abnormality, micrognathia, is shown in Alcian blue-stained specimens. *Arrow* points to the tongue in a wild-type embryo. The tongue did not develop normally in knock-out embryos. *Scale bars* indicate 1 mm. *Cyp51* wild-type, heterozygous, and knock-out embryos are designated +/+, +/−, and −/−, respectively.

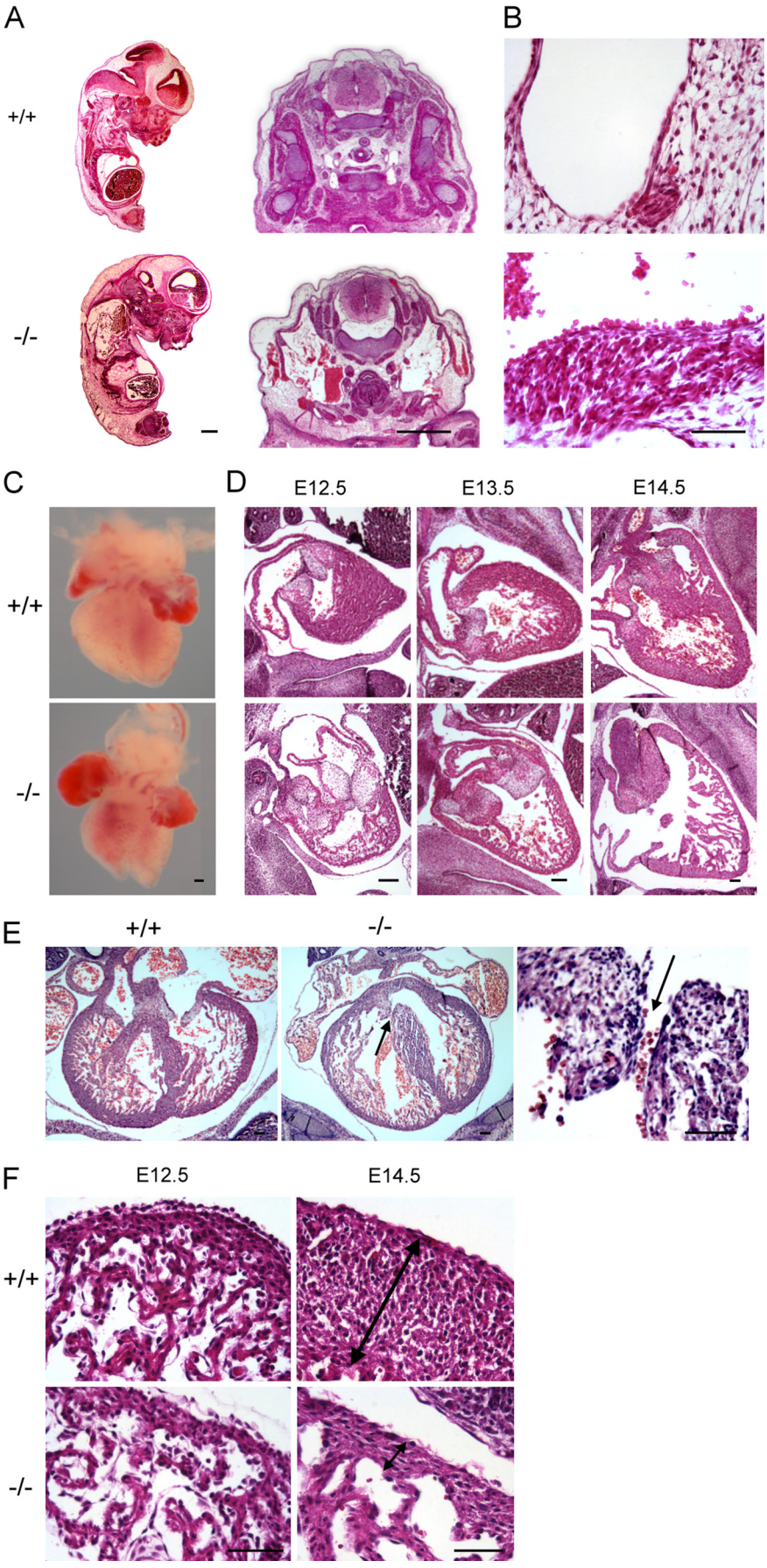
A
B
+/+
-/-
C
D
E12.5
E13.5
E14.5
+/+
-/-
E
+/+
-/-
F
E12.5
E14.5
+/+
-/-

ventricular septum, but normal structure and positioning of the great arteries (Fig. 5*C*). Histological analysis of embryos at E12.5, E13.5, and E14.5 confirmed hypoplastic development of ventricles and showed enlarged endocardial cushion tissues in the knock-out embryos compared with wild-type littermate embryos (Fig. 5*D*). In serial transversal sections, we noted ventricle septum defects in the knock-out embryos at E14.5, which were further confirmed under high-power magnification by the presence of blood cells in the communicating opening between ventricles (*arrow* in Fig. 5*E*). Examination under high-power magnification supported not only the hypoplastic myocardium at E14.5 (arrows in Fig. 5*F*), but also revealed epicardial defects between E12.5 and E14.5 with a partial lack of cells in the epicardial layer.

To investigate the potential underlying causes for the hypoplastic heart development, we analyzed proliferation and apoptosis. Proliferation was reduced in knock-out hearts at E12.5 (Fig. 6*A*), which became even more pronounced at E14.5 (Fig. 6*B*), whereas apoptosis was not different between wild-type and knock-out hearts at the investigated time points (data not shown). As histological analysis revealed abnormalities in the myocardium and epicardium, qRT-PCR analyses of several genes involved in epicardial-myocardial signaling (29) were performed. We found significantly decreased expression of retinoic X receptors (*Rxra*) and retinoic acid receptors (*Rara*) in knock-out hearts at E12.5 and E14.5 and of NK2 transcription factor related, locus 5 (*Drosophila*) (*Nkx2–5*) at E14.5. No significant change in expression levels was noted for forkhead box C1 (*Foxc1*), Wilms tumor 1 homolog (*Wt1*), vascular endothelial growth factor A (*Vegfa*), or nuclear receptor subfamily 1, group H, member 2 (*Nr1h2*) (Fig. 6*E*). In addition, lower expression of connexin 43 (*Gja1*) in the remaining epicardial cells of the knock-out hearts at E14.5 was demonstrated by qRT-PCR and confirmed with immunostaining (Fig. 6*C*). We additionally investigated expression of SHH pathway members by high sensitivity *in situ* hybridization. *Shh* and slit homolog 1 (*Drosophila Slit1*) were down-regulated in the knock-out hearts, whereas GLI-Kruppel family member GLI1 (*Gli1*) was up-regulated. Distal-less homeobox 2 (*Dlx2*) and patched homolog 1 (*Ptch1*) showed no obvious differences (supplemental Fig. S2). As *Shh*, RA, and connexin 43 (*Gja1*) are all critically involved in epicardial-myocardial signaling directing coronary vasculogenesis (for review see Ref. 29), we hypothesized that in addition to the cardiac abnormalities mentioned above, the *Cyp51* deficiency might be involved in coronary vessel formation. In support of that hypothesis, immunostaining for platelet endothelial cell adhesion molecule-1 at E12.5 revealed a significantly lower number of proliferating cardiac vessels, a difference that was even more pronounced at E14.5 (Fig. 6*D*).

DISCUSSION

We successfully developed a global knock-out mouse model of the *Cyp51* gene to gain insight into the phenotypes connected to human malformations of the ABS-like phenotype, and to further understand the importance of *de novo* cholesterol synthesis during embryogenesis. In *Cyp51* knock-out embryos, *Cyp51* mRNA was absent or significantly reduced; however, mRNA of 10 genes catalyzing various steps in the cholesterol pathway was significantly increased (Fig. 3*A*). This observation is in line with predictions that deficiencies in cholesterol or intermediates up-regulates the entire pathway in knock-out embryos to compensate for the lack of *de novo* cholesterol synthesis, which has been observed previously in other knockouts of late cholesterol synthesis such as NAD(P)-dependent steroid dehydrogenase-like knock-out mice ($Nsdhl^{-/-}$) (30). Explanation of possible mechanisms could be drawn from early literature studying effects of the CYP51 inhibitors administration. Chronic treatment with the inhibitor ketoconazole, an inhibitor of the fungal CYP51, which also inhibits the human CYP51A1 (18), mimics our *Cyp51* knock-out state. Under such conditions, enhanced hepatic 3-hydroxy-3-methylglutaryl-CoA reductase (HMGCR) activity was reported (31). Similarly, chronic administration of ketoconazole to HepG2 cells gave rise to increased HMGCR activity (32). Enhanced HMGCR activity may have been due to biological action of endogenously produced oxysterols operating via the sterol regulatory element binding transcription factor 2 (SREBF2) or the nuclear receptor subfamily 1, group H, member 3 (NR1H3) (33). The balance of natural oxysterol regulators is chronically disrupted in *Cyp51* knock-out embryos, which could cause the increase in expression of *Hmgcr* and other cholesterogenic genes, as observed in our case. An exception was *Dhcr7,* whose expression in knock-out embryos was not significantly different from the wild-type or heterozygous embryos. This was not expected because in the adult tissues and cells, transcriptional regulation of *Dhcr7* is in line with the cholesterol feedback loop and transcription factors of the sterol regulatory element binding transcription protein family. *Dhcr7* mRNA is inducible under sterol starvation or when treated with cholesterol synthesis inhibitors in the liver (34) and brain (35). Proteomic studies confirmed the increased expression of cholesterol synthesis enzymes in brains of the *Dhcr7* null mice (36). However, data from pig embryos identified *Dhcr7* as one of the imprinted, maternally expressed genes (37). It remains to be elucidated whether *Dhcr7* is also imprinted in mouse and whether this is the reason for the unchanged expression of *Dhcr7* in $Cyp51^{-/-}$ embryos. In heterozygous embryos, the *Cyp51* mRNA level was decreased by half when compared with wild-type littermates, whereas for other cholesterogenic genes no significant differ-

FIGURE 5. **Developmental heart defects in *Cyp51* knock-out embryos.** *A,* sagittal and transverse section of wild-type (+/+) and knock-out (−/−) embryos at E14.5 shows enlarged jugular lymph sac. *B,* high power magnification of jugular lymph sac endothelial lining. Endothelial cells of jugular lymph sacs appeared normal, whereas the number of surrounding smooth muscle cells was largely increased. *C,* whole mount hearts at E14.5 show normal positioning of aorta and pulmonary trunk, dilation of the atria, and a very prominent interventricular groove in knock-out embryos. *D,* histological sections of wild-type and knock-out embryo hearts at E12.5–E14.5. Note the hypoplastic development of the myocardium and the prominent endocardial cushions in knock-out embryos. *E,* transverse sections of E14.5 hearts displaying the ventricular septum defect (*arrow*). *F,* high-power magnification of the heart of E12.5 and E14.5 wild-type and knock-out embryos. Note the reduction in the compacted layer of the myocardium at E14.5 (*arrows*) and the partially detached or missing epicardial cell lining in the knock-out animals. *Scale bars* indicate 1 mm in *A* and 100 μm in *B–F*.

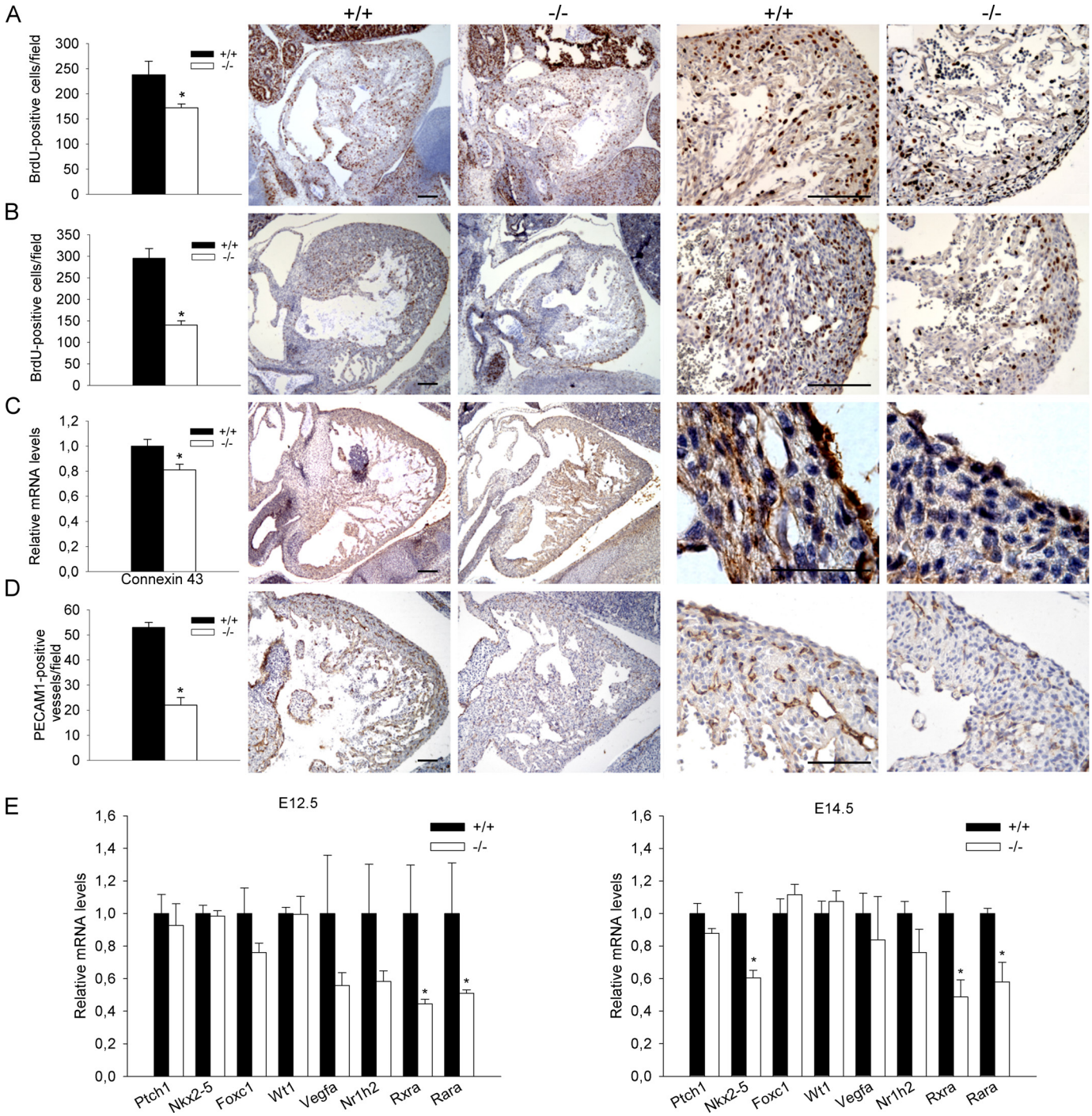

FIGURE 6. **Analyses of proliferation, apoptosis, and gene expression in hearts of *Cyp51* knock-out embryos.** *A,* BrdU immunostaining of E12.5 hearts and subsequent counting of BrdU-positive cells revealed lower proliferative activity in knock-out hearts ($n = 3$, $p < 0.05$). *B,* BrdU immunostaining of E14.5 hearts and subsequent counting of BrdU-positive cells showed an even more pronounced inhibition in cardiac cell proliferation in knock-out embryos at later stages of development ($n = 3$, *, $p < 0.05$). *C,* quantitative RT-PCR and immunostaining for connexin 43 (*Gja1*) as an important mediator of epicardial integrity and coronary vessel formation revealed reduced expression of connexin 43 in knock-out hearts at E14.5. *D,* immunostaining of hearts for platelet endothelial cell adhesion molecule-1 (*PECAM-1*, CD31) at E14.5. Note the significantly reduced number of proliferating vascular cells in *Cyp51* knock-out hearts. *Scale bars* indicate 100 μm. *E,* quantitative RT-PCR analysis of genes involved in epicardial-myocardial signaling in embryo hearts at E12.5 (*left*) and E14.5 (*right*). *Rxra* and *Rara* were down-regulated in knock-out hearts at E12.5 and E14.5, whereas *Nkx2–5* was down-regulated in E14.5. *Bars* indicate mean ± S.E.($n = 6$); *, $p < 0.05$.

ences between heterozygotes and wild-types could be detected (Fig. 3*A*). Sterol analyses of the *Cyp51* knock-out embryos show a block of cholesterol synthesis at the CYP51 enzymatic step. The two substrates of CYP51, lanosterol and 24,25-dihydrolanosterol, that are present in minute amounts in wild-type embryos, represent the only sterol intermediates that are detectable in the *Cyp51* knock-out embryos (Fig. 3*B*). Downstream from lanosterol and 24,25-dihydrolanosterol, no cholesterol intermediates were detected, suggesting that the measured cholesterol in knock-out embryos could be of maternal origin unless some as yet unknown alternative cholesterol biosynthesis pathway exists.

A role for cholesterol synthesis in development was already indicated in 1959 by data showing that ingestion of steroidal alkaloids is teratogenic (38). Such a role is also suggested by the phenotypes of the six existing mouse models with engineered mutations in cholesterol pathway genes. Loss of function of pre-squalene *Hmgcr*, mevalonate kinase (*Mvk*), and farnesyl-diphosphate farnesyltransferase 1 (*Fdft1*) genes results in early embryonic lethality, suggesting a developmental requirement for endogenous sterol(s). The *Hmgcr* knock-out (39) causes preimplantation lethality and early embryonic death was also reported for *Mvk* knock-out (40). Mice lacking *Fdft1* (41) die between E9.5 and E10.5. Our *Cyp51* knock-out is the next known model in the order of post-squalene enzymatic steps causing lethality later in development (E15.0) than the three aforementioned pre-squalene knockouts. There are four engineered knockouts of genes later in the pathway. Ablation of hydroxysteroid (17-β)-dehydrogenase 7 (*Hsd17b7*) results in embryonic lethality at E10.5 (42, 43). Early lethality of *Hsd17b7* knock-out could be explained by its additional role in estradiol synthesis. A knock-out mutation in the sterol-C5-desaturase (fungal ERG3, Δ5-desaturase) homolog (*Sc5d*) results in stillborn pups (44). Targeted disruption of *Dhcr7* in two independent studies (45, 46) led to death of pups within 24 h of birth. Two separate studies on 24-dehydrocholesterol reductase knock-out mice ($Dhcr24^{-/-}$) (47–49) demonstrate either perinatal lethality or viability to adulthood in some animals clearly indicating a genetic background effect. Our results fit into a general picture in which defects in genes active early in the pathway are early embryonic lethal, whereas those later in the pathway tend also to survive later in development, with the exception of *Hsd17b7*.

Characterization of our *Cyp51* mouse knock-out model revealed that several developmental defects resemble the ABS-like phenotype of humans such as skeletal and heart abnormalities. Skeletal abnormalities in ABS include craniosynostosis, brachycephaly, facial hypoplasia, bowed ulna or femur, synostosis of the radius, and camptodactyly. In *Cyp51* knock-out animals, we also observed facial hypoplasia, brachycephaly, and bowed and jointed bones of the extremities with camptodactyly. The reason why craniosynostosis could not be observed in our mouse model lies in the fact that they die before cranial development is complete. Syndactyly was also noticed in patients with ABS due to *POR* mutations, whereas polydactyly and hypoplastic left heart syndrome have been reported as potential teratogenic effects in response to intrauterine azole exposure. Thus, hypoplastic heart development in *Cyp51* knock-out embryos most likely corresponds to the inhibition of CYP51, similar to azole treatments in the human situation. In addition, we observed ventricular septal defects in the knock-out embryos, which are also found in some patients of ABS-like syndrome (6) together with epicardial defects and impaired cardiac vessel formation. As potential underlying mechanisms for this complex cardiac phenotype, we suggest down-regulation of *Shh*, *Rxra*, *Rara*, *Nkx2–5*, and connexin 43 (*Gja1*). Ablation of SHH signaling in the heart has been shown to result in loss of cardiac blood vessels leading to lethality due to heart failure (50). RA signaling (*Rxra*, *Rara*) in heart development has also been extensively studied using different knock-out mouse models. From these reports, it became clear that RA signaling is involved in differentiation of embryonic ventricular cardiomyocytes (51) and is necessary to avoid cardiac hypoplasia (52) and epicardial and coronary vessel defects (53). Growth of $Nkx2–5^{-/-}$ mutant hearts arrests during the looping heart stage when a complete lack of ventricle septum formation, severe cardiac hypoplasia, and underdevelopment of the outflow tract (54, 55) are observed. Connexin 43 deficiency results in partial detachment of the epicardium and disturbed coronary vessel formation (56, 57). Down-regulation of all the above mentioned genes in the hearts of *Cyp51* knock-out embryos could be expected to contribute to the observed cardiac phenotype. However, the exact molecular mechanism leading to this down-regulation in the *Cyp51*-deficient hearts remains to be determined.

ABS has been most frequently associated with recessive mutations in *POR* (ABS1 form), but also in some cases with dominant mutations in *FGFR2* (ABS2 form). A mouse knock-out of the *FGFR2* ortholog does not model ABS2 in humans as the heterozygote mice are normal (no dominant effect), whereas homozygous nulls die at the blastocyst stage (58). Two mouse knockouts exist for the *Por* gene and exhibit a wide range of defects including neural tube, eye, heart, limb, and retarded growth, and embryos do not survive beyond E10.5 (59) or E13.5 (60). Although some developmental abnormalities were similar to the ones reported in our *Cyp51* knock-out study, it is clear that *Por* null embryos have a broader range of developmental abnormalities possibly because *Por* is involved as electron donor in multiple biochemical pathways (5). Additionally, the *Por* knock-out may not be the most suitable animal model for ABS1 because there is only one copy of *Por* in the mouse genome (62), whereas in humans, the *POR* gene maps to a duplication region of chromosome 7 (61) likely providing some redundancy. By generating a knock-out model of the *Cyp51* gene, we therefore generated a genetic inactivation model that can help to characterize the importance of *Cyp51* in the observed ABS-like phenotype in humans and indicate the possibility of a new form of ABS syndrome where mutations in the human orthologous gene *CYP51A1* may be involved.

A lesson from the human cholesterol biosynthesis syndromes and mouse knockouts is that a complete inhibition of cholesterol synthesis results in embryonic or early postnatal lethality. However, the time when lethality occurs depends on the step of the pathway that a particular gene catalyzes. The earlier the gene acts in the pathway, the earlier embryonic lethality occurs. It still remains unclear whether the phenotypes reported are a consequence of cholesterol deficiency, accumulation of intermediates upstream of the knock-out gene, lack of intermediates downstream of the knock-out, perturbations of pathways branching from the "main" cholesterol pathway, or an interaction of these aforementioned factors. Perturbations in levels of sterol intermediates and their novel oxysterol metabolites have already been demonstrated to have a role in the pathophysiology of embryo development. It has been shown recently that phenotypes like micrognathia, cleft palate, and limb malformations are a direct consequence of oxysterol accumulation due to the activity of sterol 27-hydroxylase CYP27A1), rather than altered cholesterol levels (reviewed in

Ref. 23). Although future studies may find some common mechanisms to explain developmental phenotypes of cholesterol biosynthesis gene knock-out or deficiency models, it is also likely that some models have their own underlying molecular basis and that one unifying mechanism may not exist. Our comparative study with cholesterol human syndromes reveals that the *Cyp51* knock-out phenotype resembles many features of ABS and can hence serve as an animal model for this syndrome. As we developed a conditional $Cyp51^{flox}$ allele, this enables development of conditional knockouts to study tissue- or time-specific effects of CYP51 deficiency or generating partial loss of *Cyp51* function to provide hypomorphic ABS models suitable for studies in adult animals.

Acknowledgments—We thank G. Fishell for in situ hybridization probes. We also thank Dr. I. Bjorkhem, Karolinska Institute, for providing help in GS-MS measurements and T. Rezen for help in the initial studies. We also acknowledge a travel grant for Slovenia-France cooperation in science and technology, co-financed through program "Proteus" by the Slovenian Research Agency and French agency EGIDE.

REFERENCES

1. Kenworthy, A. (2002) *Trends Biochem. Sci.* **27,** 435–437
2. Porter, J. A., Young, K. E., and Beachy, P. A. (1996) *Science* **274,** 255–259
3. Beachy, P. A., Cooper, M. K., Young, K. E., von Kessler, D. P., Park, W. J., Hall, T. M., Leahy, D. J., and Porter, J. A. (1997) *Cold Spring Harbor Symp. Quant. Biol.* **62,** 191–204
4. Huq, M. D., Tsai, N. P., Gupta, P., and Wei, L. N. (2006) *EMBO J.* **25,** 3203–3213
5. Horvat, S., McWhir, J., and Rozman, D. (2011) *Drug Metab. Rev.* **43,** 69–90
6. Porter, F. D., and Herman, G. E. (2011) *J. Lipid Res.* **52,** 6–34
7. Antley, R. M., and Bixler, D. (1975) *Birth Defects Orig. Art. Ser.* **XI**, 397–401
8. Flück, C. E., Tajima, T., Pandey, A. V., Arlt, W., Okuhara, K., Verge, C. F., Jabs, E. W., Mendonça, B. B., Fujieda, K., and Miller, W. L. (2004) *Nat. Genet.* **36,** 228–230
9. McGlaughlin, K. L., Witherow, H., Dunaway, D. J., David, D. J., and Anderson, P. J. (2010) *J. Craniofac. Surg.* **21,** 1560–1564
10. Fukami, M., Horikawa, R., Nagai, T., Tanaka, T., Naiki, Y., Sato, N., Okuyama, T., Nakai, H., Soneda, S., Tachibana, K., Matsuo, N., Sato, S., Homma, K., Nishimura, G., Hasegawa, T., and Ogata, T. (2005) *J. Clin. Endocrinol. Metab.* **90,** 414–426
11. Lee, B. E., Feinberg, M., Abraham, J. J., and Murthy, A. R. K. (1992) *Pediatr. Infect. Dis. J.* **11,** 1062–1064
12. Pursley, T. J., Blomquist, I. K., Abraham, J., Andersen, H. F., and Bartley, J. A. (1996) *Clin. Infect. Dis.* **22,** 336–340
13. Aleck, K. A., and Bartley, D. L. (1997) *Am. J. Med. Genet.* **72,** 253–256
14. Cragun, D. L., Trumpy, S. K., Shackleton, C. H., Kelley, R. I., Leslie, N. D., Mulrooney, N. P., and Hopkin, R. J. (2004) *Am. J. Med. Genet.* **129A,** 1–7
15. Rezen, T., Debeljak, N., Kordis, D., and Rozman, D. (2004) *J. Mol. Evol.* **59,** 51–58
16. Strömstedt, M., Rozman, D., and Waterman, M. R. (1996) *Arch. Biochem. Biophys.* **329,** 73–81
17. Debeljak, N., Horvat, S., Vouk, K., Lee, M., and Rozman, D. (2000) *Arch. Biochem. Biophys.* **379,** 37–45
18. Lamb, D. C., Kelly, D. E., Waterman, M. R., Stromstedt, M., Rozman, D., and Kelly, S. L. (1999) *Yeast* **15,** 755–763
19. Magin, T. M., McWhir, J., and Melton, D. W. (1992) *Nucleic Acids Res.* **20,** 3795–3796
20. Jegalian, B. G., and De Robertis, E. M. (1992) *Cell* **71,** 901–910
21. Wagner, N., Wagner, K. D., Theres, H., Englert, C., Schedl, A., and Scholz, H. (2005) *Genes Dev.* **19,** 2631–2642
22. Wagner, K. D., Wagner, N., Bondke, A., Nafz, B., Flemming, B., Theres, H., and Scholz, H. (2002) *FASEB J.* **16,** 1117–1119
23. Fakheri, R. J., and Javitt, N. B. (2011) *Steroids* **76,** 211–215
24. Wagner, K. D., Wagner, N., Wellmann, S., Schley, G., Bondke, A., Theres, H., and Scholz, H. (2003) *FASEB J.* **17,** 1364–1366
25. Acimovic, J., Lovgren-Sandblom, A., Monostory, K., Rozman, D., Golicnik, M., Lutjohann, D., and Bjorkhem, I. (2009) *J. Chromatogr. B* **877,** 2081–2086
26. Vandesompele, J., De Preter, K., Pattyn, F., Poppe, B., Van Roy, N., De Paepe, A., and Speleman, F. (2002) *Genome Biol.* **3,** RESEARCH0034
27. Kosir, R., Acimovic, J., Golicnik, M., Perse, M., Majdic, G., Fink, M., and Rozman, D. (2010) *BMC Mol. Biol.* **11,** 60
28. Hyett, J. A. (2002) *Prenat. Diagn.* **22,** 864–868
29. Olivey, H. E., and Svensson, E. C. (2010) *Circ. Res.* **106,** 818–832
30. Cunningham, D., Swartzlander, D., Liyanarachchi, S., Davuluri, R. V., and Herman, G. E. (2005) *J. Lipid Res.* **46,** 1150–1162
31. Gibbons, G. F. (2002) *Lipids* **37,** 1163–1170
32. Kempen, H. J., van Son, K., Cohen, L. H., Griffioen, M., Verboom, H., and Havekes, L. (1987) *Biochem. Pharmacol.* **36,** 1245–1249
33. Javitt, N. B. (2008) *Steroids* **73,** 149–157
34. Kim, J. H., Lee, J. N., and Paik, Y. K. (2001) *J. Biol. Chem.* **276,** 18153–18160
35. Lauth, M., Rohnalter, V., Bergström, A., Kooshesh, M., Svenningsson, P., and Toftgård, R. (2010) *Mol. Pharmacol.* **78,** 486–496
36. Jiang, X. S., Backlund, P. S., Wassif, C. A., Yergey, A. L., and Porter, F. D. (2010) *Mol. Cell. Proteomics* **9,** 1461–1475
37. Bischoff, S. R., Tsai, S., Hardison, N., Motsinger-Reif, A. A., Freking, B. A., Nonneman, D., Rohrer, G., and Piedrahita, J. A. (2009) *Biol. Reprod.* **81,** 906–920
38. Binns, W., Thacker, E. J., James, L. F., and Huffman, W. T. (1959) *J. Am. Vet. Med. Assoc.* **134,** 180–183
39. Ohashi, K., Osuga, J., Tozawa, R., Kitamine, T., Yagyu, H., Sekiya, M., Tomita, S., Okazaki, H., Tamura, Y., Yahagi, N., Iizuka, Y., Harada, K., Gotoda, T., Shimano, H., Yamada, N., and Ishibashi, S. (2003) *J. Biol. Chem.* **278,** 42936–42941
40. Hager, E. J., Tse, H. M., Piganelli, J. D., Gupta, M., Baetscher, M., Tse, T. E., Pappu, A. S., Steiner, R. D., Hoffmann, G. F., and Gibson, K. M. (2007) *J. Inherit. Metab. Dis.* **30,** 888–895
41. Tozawa, R., Ishibashi, S., Osuga, J., Yagyu, H., Oka, T., Chen, Z., Ohashi, K., Perrey, S., Shionoiri, F., Yahagi, N., Harada, K., Gotoda, T., Yazaki, Y., and Yamada, N. (1999) *J. Biol. Chem.* **274,** 30843–30848
42. Jokela, H., Rantakari, P., Lamminen, T., Strauss, L., Ola, R., Mutka, A. L., Gylling, H., Miettinen, T., Pakarinen, P., Sainio, K., and Poutanen, M. (2010) *Endocrinology* **151,** 1884–1892
43. Shehu, A., Mao, J., Gibori, G. B., Halperin, J., Le, J., Devi, Y. S., Merrill, B., Kiyokawa, H., and Gibori, G. (2008) *Mol. Endocrinol.* **22,** 2268–2277
44. Krakowiak, P. A., Wassif, C. A., Kratz, L., Cozma, D., Kovárová, M., Harris, G., Grinberg, A., Yang, Y., Hunter, A. G., Tsokos, M., Kelley, R. I., and Porter, F. D. (2003) *Hum. Mol. Genet.* **12,** 1631–1641
45. Fitzky, B. U., Moebius, F. F., Asaoka, H., Waage-Baudet, H., Xu, L., Xu, G., Maeda, N., Kluckman, K., Hiller, S., Yu, H., Batta, A. K., Shefer, S., Chen, T., Salen, G., Sulik, K., Simoni, R. D., Ness, G. C., Glossmann, H., Patel, S. B., and Tint, G. S. (2001) *J. Clin. Invest.* **108,** 905–915
46. Wassif, C. A., Zhu, P., Kratz, L., Krakowiak, P. A., Battaile, K. P., Weight, F. F., Grinberg, A., Steiner, R. D., Nwokoro, N. A., Kelley, R. I., Stewart, R. R., and Porter, F. D. (2001) *Hum. Mol. Genet.* **10,** 555–564
47. Wechsler, A., Brafman, A., Shafir, M., Heverin, M., Gottlieb, H., Damari, G., Gozlan-Kelner, S., Spivak, I., Moshkin, O., Fridman, E., Becker, Y., Skaliter, R., Einat, P., Faerman, A., Björkhem, I., and Feinstein, E. (2003) *Science* **302,** 2087–2087
48. Mirza, R., Hayasaka, S., Takagishi, Y., Kambe, F., Ohmori, S., Maki, K., Yamamoto, M., Murakami, K., Kaji, T., Zadworny, D., Murata, Y., and Seo, H. (2006) *J. Invest. Dermatol.* **126,** 638–647
49. Mirza, R., Qiao, S., Murata, Y., and Seo, H. (2009) *Am. J. Dermatopathol.* **31,** 446–452
50. Lavine, K. J., Kovacs, A., and Ornitz, D. M. (2008) *J. Clin. Invest.* **118,** 2404–2414
51. Kastner, P., Messaddeq, N., Mark, M., Wendling, O., Grondona, J. M.,

Ward, S., Ghyselinck, N., and Chambon, P. (1997) *Development* **124,** 4749–4758
52. Sucov, H. M., Dyson, E., Gumeringer, C. L., Price, J., Chien, K. R., and Evans, R. M. (1994) *Genes Dev.* **8,** 1007–1018
53. Merki, E., Zamora, M., Raya, A., Kawakami, Y., Wang, J., Zhang, X., Burch, J., Kubalak, S. W., Kaliman, P., Belmonte, J. C., Chien, K. R., and Ruiz-Lozano, P. (2005) *Proc. Natl. Acad. Sci. U.S.A.* **102,** 18455–18460
54. Lyons, I., Parsons, L. M., Hartley, L., Li, R., Andrews, J. E., Robb, L., and Harvey, R. P. (1995) *Genes Dev.* **9,** 1654–1666
55. Tanaka, M., Wechsler, S. B., Lee, I. W., Yamasaki, N., Lawitts, J. A., and Izumo, S. (1999) *Development* **126,** 1439–1450
56. Rhee, D. Y., Zhao, X. Q., Francis, R. J., Huang, G. Y., Mably, J. D., and Lo, C. W. (2009) *Development* **136,** 3185–3193
57. Walker, D. L., Vacha, S. J., Kirby, M. L., and Lo, C. W. (2005) *Dev. Biol.* **284,** 479–498
58. Arman, E., Haffner-Krausz, R., Chen, Y., Heath, J. K., and Lonai, P. (1998) *Proc. Natl. Acad. Sci. U.S.A.* **95,** 5082–5087
59. Otto, D. M., Henderson, C. J., Carrie, D., Davey, M., Gundersen, T. E., Blomhoff, R., Adams, R. H., Tickle, C., and Wolf, C. R. (2003) *Mol. Cell. Biol.* **23,** 6103–6116
60. Shen, A. L., O'Leary, K. A., and Kasper, C. B. (2002) *J. Biol. Chem.* **277,** 6536–6541
61. Peoples, R., Franke, Y., Wang, Y. K., Pérez-Jurado, L., Paperna, T., Cisco, M., and Francke, U. (2000) *Am. J. Hum. Genet.* **66,** 47–68
62. Simmons, D. L., Lalley, P. A., and Kasper, C. B. (1985) *J. Biol. Chem.* **260,** 515–521